


# A Thallium-Based Screening Procedure to Identify Molecules That Modulate the Activity of Ca<sup>2+</sup>-Activated Monovalent Cation-Selective Channels

SLAS Discovery  
1–12  
© 2018 Society for Laboratory  
Automation and Screening  
DOI: 10.1177/2472555217748932  
slasdisc.sagepub.com  


Koenraad Philippaert<sup>1,2,3</sup> , Sara Kerselaers<sup>1,2,3</sup>, Thomas Voets<sup>1,2,3</sup>,  
and Rudi Vennekens<sup>1,2,3</sup>

## Abstract

TRPM5 functions as a calcium-activated monovalent cation-selective ion channel and is expressed in a variety of cell types. Dysfunction of this type of channel has been recently implied in cardiac arrhythmias, diabetes, and other pathologies. Therefore, a growing interest has emerged to develop the pharmacology of these ion channels. We optimized a screening assay based on the thallium flux through the TRPM5 channel and a fluorescent thallium dye as a probe for channel activity. We show that this assay is capable of identifying molecules that inhibit or potentiate calcium-activated monovalent cation-selective ion channels.

## Keywords

fluorescence methods, cell-based assays, high-content screening, ion channels, natural products screening

## Introduction

TRP channels are a family of 28 mammalian cation channels involved in calcium signaling and the electrical activity of a variety of cell types. Dysfunction of TRP channels has been linked to the etiology of several diseases, such as polycystic kidney disease, diabetes, and cardiac conductivity disorders. TRPM4 and TRPM5 are functionally distinct members of this family, as they are the only two TRP channels that are both activated by an increase in intracellular calcium and selective for monovalent cations.<sup>1</sup> To date, they are the only molecular candidates for this class of cation channels.<sup>2</sup> Ion channel activity with properties reminiscent of those of TRPM4 or TRPM5 was first described in cardiac myocytes<sup>3</sup> but has since been described in a wide range of excitable and nonexcitable cells.

TRPM4 is widely expressed with abundant expression in the cardiac muscle, prostate, colon, and kidneys.<sup>4</sup> Recent research revealed an important function for TRPM4 in the cardiovascular system, the immune system, and the central nervous system.<sup>3,5,6</sup> Mutations in the TRPM4 gene are associated with cardiac conduction disorders, such as progressive familial heart block and Brugada syndrome.<sup>7–9</sup> It has been suggested that TRPM4 inhibitors might be useful for the treatment of these conditions. TRPM5, on the other hand, has a distinct expression pattern in chemosensitive cells throughout the body. Recently, our group described the

functional role of this channel in insulin-secreting pancreatic  $\beta$ -cells. Potentiation of TRPM5 with steviol glycosides stimulates glucose-induced insulin release, and thereby increases postprandial insulin levels.<sup>10,11</sup> We showed that chronic treatment of mice with steviol glycosides prevents the development of hyperglycemia in high-fat-diet-fed mice,<sup>12</sup> suggesting that TRPM5 modulators may potentially be useful as insulin secretagogue medication. Furthermore, TRPM5 plays an essential role in the taste transduction signaling in the type II taste receptor cells in the taste buds.<sup>10,13–15</sup> TRPM5 is an essential downstream target of taste receptor activation, and is thus essential for sweet, bitter, or umami taste perception.<sup>16</sup> We showed that TRPM5 potentiation by

<sup>1</sup>Laboratory of Ion Channel Research, Department of Cellular and Molecular Medicine, KULeuven, Leuven, Vlaams Brabant, Belgium

<sup>2</sup>TRP Research Platform Leuven (TRPLe), KULeuven, Leuven, Belgium

<sup>3</sup>VIB Center for Brain & Disease Research, Leuven, Belgium

Received May 18, 2017, and in revised form Nov 27, 2017. Accepted for publication Nov 28, 2017.

Supplementary material is available online with this article.

## Corresponding Author:

Koenraad Philippaert, Laboratory of Ion Channel Research, Department of Cellular and Molecular Medicine, KULeuven, Herestraat 49 Box 802, Leuven, Vlaams Brabant 3000, Belgium.  
Email: Koenraad.Phillippaert@kuleuven.vib.be

steviol intensifies the taste response of mice for sweet, bitter, and umami compounds.<sup>11</sup> Currently, the number of known compounds that selectively modify this type of ion channels is very limited.<sup>11,17–21</sup> These compounds would be useful to clarify the physiological role of the channel but, as outlined above, could also be useful for the development of novel drugs.<sup>22</sup>

TRP channels have been targets in fluorescent screening assays before. Methods have been developed that probe  $\text{Ca}^{2+}$  or  $\text{Mn}^{2+}$  flux through TRPA1, TRPC4, TRPM7, TRPM8, or TRPV1 with Fluo-4 or FURA2.<sup>23–27</sup> The activity of TRPM4 and TRPM5 cannot be assessed with a  $\text{Ca}^{2+}$ -based screening method since they are monovalent cation-selective channels and impermeable to  $\text{Ca}^{2+}$ . Fluorescent membrane potential dyes and  $\text{Na}^+$ -sensitive dyes could be useful in this regard.<sup>28</sup> However,  $\text{Na}^+$  dyes, such as SBFI, CoroNa, and Asante, have a poor signal-to-noise ratio due to the relatively small changes in intracellular  $\text{Na}^+$  concentration in such an assay. Voltage-sensitive dyes are sensitive to any ion channel-mediated event that changes the membrane potential of the cell, and are therefore notorious for high false-positive rates. An intriguing alternative is the Thallo dye. This is a thallium ( $\text{Tl}^+$ )-sensitive fluorescent dye with peak emission at 515 nm after excitation at 490 nm, whose fluorescence increases upon binding of  $\text{Tl}^+$ . Several Thallo-based screening methods exploit the permeability of cation channels for  $\text{Tl}^+$ , and this approach has proven successful for  $\text{K}^+$  or  $\text{Na}^+$  channels  $K_{\text{Ca}}3.1$ ,  $K_{\text{ir}}4.1$ , and  $\text{Na}_v1.7$ .<sup>29–31</sup> Here, we demonstrate that Thallo-mediated detection of  $\text{Tl}^+$  influx into the cell is a suitable fluorescence-based screening method to probe TRPM5 and TRPM4 activity.

## Materials and Methods

### Electrophysiology

Voltage clamp recordings were monitored using an EPC-10 patch clamp amplifier controlled by a Windows PC and PatchMaster v2x73.2. Patch pipettes were pulled from Vitrex capillary tubes using a DMZ-Universal puller and had a resistance between 2 and 5 M $\Omega$ . An Ag-AgCl wire was used as the pipette and reference electrode. Membrane capacitive transients were electronically compensated. Between 50% and 70% of the series resistance was electronically compensated in order to minimize voltage errors. We used the whole-cell patch clamp configuration. A linear stimulation protocol from  $-110$  to  $+110$  mV in 300 ms was applied to the cells with a frequency of 1 Hz. Our standard bath solution contained (mM) 150 NaCl, 6 KCl, 1.5  $\text{CaCl}_2$ , 1  $\text{MgCl}_2$ , 10 glucose, and 10 HEPES titrated with 1 M NaOH to a pH of 7.4. For assessing the thallium permeability of the channel, we changed to a bath solution containing (mM) 100  $\text{Na}_2\text{SO}_4$ , 1  $\text{MgSO}_4$ , and 10 HEPES with a pH of 7.4 ( $\text{Ca}(\text{OH})_2$ ) and alternated perfusion of the thallium

solution containing (mM) 100  $\text{Ti}_2\text{SO}_4$ , 1  $\text{MgSO}_4$ , and 10 HEPES at pH 7.4 ( $\text{Ca}(\text{OH})_2$ ). The pipette solution contained (mM) 50 NaCl, 100 *N*-methyl-D-glucamine, 10 HEPES, 10 ethylene glycol tetraacetic acid (EGTA), 4  $\text{K}_2\text{ATP}$ , and 8.62  $\text{CaCl}_2$ , titrated to a pH of 7.2 with HCl. The free  $\text{Ca}^{2+}$  concentration was 1  $\mu\text{M}$ . The standard bath solution was used for establishing the cell-attached configuration, after which the  $\text{Na}_2\text{SO}_4$  was perfused before breaking into the cell for whole-cell patch. During TRPM5 activity, the extracellular sodium was briefly replaced by thallium in multiple events. Inward currents and reversal potential during  $\text{Na}^+$  or  $\text{Tl}^+$  perfusion were compared with a paired sample *t* test.

### Microfluorimetry

NaCl-based extracellular solutions were omitted because of the limited water solubility of  $\text{TlCl}$ . We used a gluconate-based extracellular buffer that yielded satisfying results on a potassium channel compound screening.<sup>32</sup> We seeded TRPM5-expressing cells on polylysine-coated coverslips. The cells were loaded for 30 min with 0.96  $\mu\text{M}$  Thallo dye in culture medium at 37 °C, after which they were placed on an upright fluorescence microscope equipped with a multi-channel gravity-controlled perfusion system. Fluorescence was followed every second, and solutions were perfused as indicated (see **Suppl. Fig. S1**). Excitation was done with a polychrome V light source and image acquisition with an Andor iXon 888 camera controlled with the TILL photonics Live Acquisition 2.3.0.18 software.

### Cell Culture

A HEK-293 cell line expressing TRPM5 or TRPM4 was created using the FLP-In system (Life Technologies, Waltham, MA) according to the manufacturer's protocol. Cells were cultured in Dulbecco's modified Eagle's medium (DMEM) supplemented with 1% NEAA, 10,000 U/mL penicillin-streptomycin, 10 mM GlutaMAX, and 100  $\mu\text{g}/\text{mL}$  hygromycin. All cell culture reagents were purchased from Gibco, Life Technologies. Cells were passaged twice a week and kept in a humidified incubator at 37 °C and 10%  $\text{CO}_2$ . The  $\mu\text{Clear}$  bottom black 96-well plates (Greiner Bio-One, Monroe, NC) were coated with 0.01% poly-L-lysine (Sigma, St. Louis, MO) and washed with divalent-ion-free phosphate-buffered saline (PBS) (Gibco). Before the assay (24–30 h), the cells were harvested by trypsinization and washed in culture medium. Cells were counted using a standard Bürker counting chamber and 10,000 cells per well were plated on the  $\mu\text{Clear}$  bottom black 96-well plates in 100  $\mu\text{L}$  of medium per well. For microfluorimetry and patch clamp experiments, the cells were seeded onto poly-L-lysine-coated coverslips and incubated for 2–6 h before the experiment. The coverslips were mounted onto an inverted microscope equipped with a multichannel perfusion system.

## Buffer Optimization

To optimize the extracellular ionic buffer conditions, a selection of buffers was made. We used gluconate, aspartate, or nitrate as the main anion in our buffer solution, and permuted the main cation to  $\text{Na}^+$  and  $\text{K}^+$ . These six buffer conditions consisted of 138 mM  $\text{KNO}_3$  (or the appropriate substitution of main anion or cation) and (in mM) 1.3  $\text{CaSO}_4$ , 0.8  $\text{MgSO}_4$ , 5.6 D-glucose, and 20 HEPES, titrated to pH 7.3 using 1 M KOH or NaOH based on the main cation (chemicals from Sigma). We used thallium concentrations of 0, 0.2, 2, and 10 mM to screen for the optimal concentration.

## Compound Preparation

Stock solutions from all compounds were made in DMSO with a concentration of  $\geq 10$  mM. The compounds were transferred into V-bottom 96-well plates at a concentration of 100  $\mu\text{M}$ , and a duplicate for each compound was included on the same plate, together with positive and negative controls. The plates were designed with a control condition in every column to normalize the signals. Duplicate samples were located six columns to the right of the first sample, making two identical halves on a 96-well plate.

The buffer solution to dilute the compounds contains (mM) 138  $\text{KNO}_3$ , 1.3  $\text{CaSO}_4$ , 0.8  $\text{MgSO}_4$ , 10  $\text{Ti}_2\text{SO}_4$ , 5.6 D-glucose, 0.02 ionomycin (Enzo, New York, NY), and 20 HEPES, titrated to pH 7.3 using 1 M KOH. A 2 mM stock solution of ionomycin in ethanol was used. Positive control conditions were free of compound and only contained solvent. Negative control conditions contained buffer without ionomycin, supplemented with 1% DMSO as solvent control for the compound conditions. The compound plates were prepared 12–72 h before the assay, stored at  $-20^\circ\text{C}$ , and defrosted to room temperature shortly before the assay.

## Screening Procedure

The cell culture medium on the 96-well plate was removed and replaced with 100  $\mu\text{L}$  of culture medium supplemented with 2.5 mM probenecid (Sigma) and 0.96  $\mu\text{M}$  Thallos dye (TEFLabs, Austin, TX) and 0.2  $\mu\text{g}/\text{mL}$  Pluronic F-127 (Invitrogen, Waltham, MA). Cells were incubated with the dye for 30 min in a humidified incubator at  $37^\circ\text{C}$  and 10%  $\text{CO}_2$ . After incubation, the loading medium was discarded and 135  $\mu\text{L}$  of assay buffer was added to each well. The screening occurred on a FlexStation3 (Molecular Devices, Sunnyvale, CA) fluorescent microplate reader, controlled with the SoftMax Pro 5 software. The FlexStation3 reads the full time course on the first column before continuing to the next column. With a positive control in each column, we can control for the time-dependent variation within one assay. Fluorescence emission of the Thallos dye was

followed at 515 nm after excitation at 490 nm. The protocol consists of a 20 s baseline measurement, after which 15  $\mu\text{L}$  out of the compound plate was transferred onto the cell plate to obtain a 1/10 dilution that results in a final compound concentration of 10  $\mu\text{M}$ . After addition of the compound, the fluorescence signal was followed for another 50 s. Every plate was evaluated on correlation between duplicates and  $Z'$  factor to identify the power of the assay.<sup>33</sup> Only plates with a  $Z'$  of  $>0.5$  and a Pearson's correlation within the plate of  $>0.85$  were deemed acceptable.

## Data Analysis

We used a custom procedure script in Igor Pro 6.34 (Wavemetrics, Portland, OR) to analyze the obtained data. From every trace, the amplitude was calculated as the difference between the average baseline value at 0–16 s and the maximal amplitude as the average between 50 and 70 s.

The relative amplitude is calculated as  $amp = \left\langle \frac{F - F_0}{F_{100\%} - F_0} \right\rangle$ ,

where 100% is the compound-free control condition in the same column. The relative maximal rate of fluorescence increase is based on the first time derivative of the fluorescence signal:  $rate = \left\langle \frac{(dF)_{MAX}}{(dF_{100\%})_{MAX}} \right\rangle$ , where  $dF$  is the first

derivative of the fluorescence trace to time, and  $MAX$  indicates the maximal value reached during the acute addition phase ( $t = 11$ – $30$  s). These values are normalized to the positive control values on the plate. The reported values are the average and standard deviation (SD) of the two duplicates of each compound. The  $Z'$  factor was calculated as

$$Z' = 1 - \frac{3(\sigma_p + \sigma_n)}{|\hat{\mu}_p - \hat{\mu}_n|}, \text{ with } \sigma_p \text{ the SD of the positive control}$$

amplitudes,  $\sigma_n$  the SD of the negative control amplitudes, and  $\mu_p$  and  $\mu_n$  the average amplitudes of the positive and negative controls, respectively. We calculated  $Z$  as

$$Z = 1 - \frac{3(\sigma_c + \sigma_s)}{|\hat{\mu}_c - \hat{\mu}_s|}, \text{ with } \sigma_s \text{ and } \mu_s \text{ the SD and average of the}$$

sample and  $\sigma_c$  and  $\mu_c$  the SD and average of the control conditions.<sup>33</sup> The signal-to-noise ratio was calculated as  $S/N = \frac{\mu_c - \mu_{bg}}{SD_{bg}}$ , with  $\mu_c$  the mean of the control,  $\mu_{bg}$  the

mean of the background, and  $SD_{bg}$  the SD of the background conditions. We used OriginPro 8.6 for statistics and graph design.

## Results and Discussion

At the onset of this study, it remained to be shown that (1) TRPM5 is thallium permeable, (2) the dominant thallium influx occurs through TRPM5 in HEK cells expressing the channel, (3) the thallium influx rate is significantly influenced

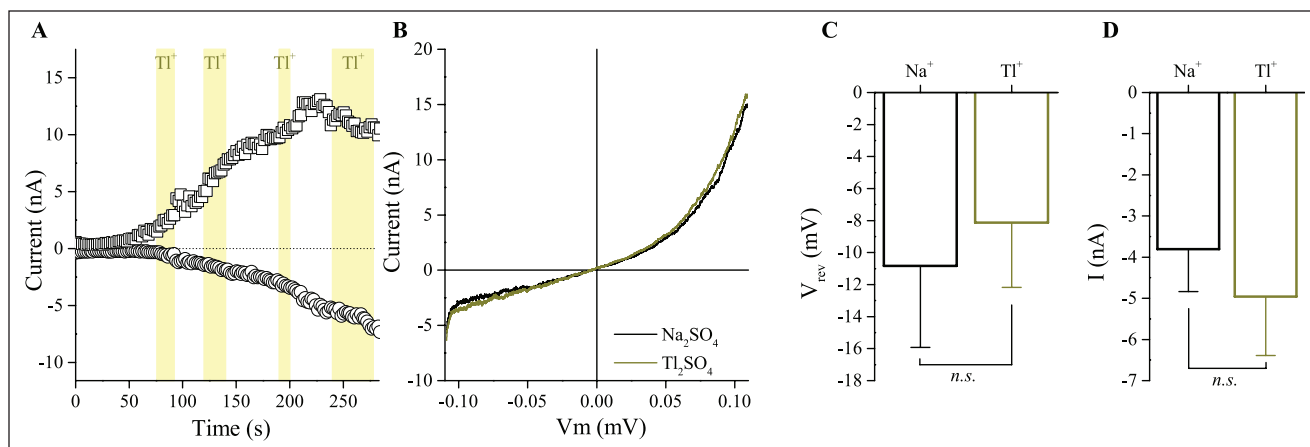


**Figure 1.** Thallium permeability of TRPM5. **(A)** Time trace of in- and outward currents at  $\pm 100$  mV in  $\text{Na}_2\text{SO}_4$  or  $\text{TI}_2\text{SO}_4$  (yellow). **(B)** Example IV traces with  $\text{TI}^+$  or  $\text{Na}^+$  as extracellular monovalent cation. **(C)** Reversal potential and **(D)** inward current during perfusion with  $\text{Na}_2\text{SO}_4$  or  $\text{TI}_2\text{SO}_4$  ( $n = 8$  cells).

by modulating TRPM5 activity, and (4) the protocol optimized for TRPM5 could also be used on other channels with similar properties, for instance, TRPM4.

### TRPM5 Is Thallium Permeable

We first explored the permeability of TRPM5 for  $\text{TI}^+$  in whole-cell patch clamp experiments, using HEK cells that stably express murine TRPM5. TRPM5 was activated by including  $10 \mu\text{M}$   $\text{Ca}^{2+}$  in the pipette solution. As shown in **Figure 1**,  $\text{Ca}^{2+}$ -induced currents in these cells were indistinguishable when measured in a bath solution containing  $\text{Na}^+$  or  $\text{TI}^+$  as the extracellular cation (**Fig. 1 A, B**). The inward current amplitude and the reversal potential are not different (**Fig. 1 C, D**, mean  $\pm$  SEM from 8 cells). Notably, these experiments were performed using  $\text{SO}_4^{2-}$  as extracellular anion, to avoid precipitation of  $\text{TICl}$ . For the same reason, we used only brief application periods of  $\text{TI}^+$  to the cells, since longer application times caused  $\text{TI}^+$  accumulation in the cells and the formation of intracellular  $\text{TICl}$  crystals. Taken together, these data demonstrate that TRPM5 is permeable for  $\text{TI}^+$ .

### Thallium Influx Changes Thallos Fluorescence in HEK TRPM5 Cells

Microfluorimetry measurements of individual TRPM5-expressing HEK cells loaded with Thallos revealed changes in fluorescence upon addition of  $\text{TI}^+$  to the extracellular medium, even without an elevation of  $[\text{Ca}^{2+}]_i$  that would activate TRPM5 (**Suppl. Fig. S1A**). This indicates that a background  $\text{TI}^+$  influx is present in these cells. Upon addition of ionomycin, causing a rapid intracellular calcium increase and activation of TRPM5, we observed a further increase in the Thallos fluorescence (**Suppl. Fig. S1B**). When simultaneously applying thallium and ionomycin to

the bath solution, we observed a faster maximum rate of fluorescence increase than that observed by applying thallium alone (**Suppl. Fig. S1C**). Clearly, the TRPM5-dependent fluorescence signal was in these conditions fairly small compared with the background signal.

To minimize TRPM5-independent thallium influx and in order to achieve high TRPM5-dependent thallium influx, we tested several experimental conditions. We varied the main extracellular buffer components: either  $\text{Na}^+$  or  $\text{K}^+$  as cation and gluconate ( $\text{Glu}^-$ ), nitrate ( $\text{NO}_3^-$ ), or aspartate ( $\text{Asp}^-$ ) as anion.  $\text{Cl}^-$  was excluded, as  $\text{TICl}$  is only soluble to a very limited extent. To determine the background fluorescence signal, control experiments were performed in HEK cells not expressing TRPM5. Both HEK TRPM5 and control HEK cells were tested in the presence or absence of ionomycin ( $2 \mu\text{M}$ ), which will increase intracellular  $\text{Ca}^{2+}$  and thereby activate TRPM5. The extracellular solution was supplemented with either 0.2, 2, or 10 mM  $\text{TI}^+$ . All conditions were screened in 96-well plates, using a FlexStation3. The results are summarized in **Figure 2** and **Supplemental Figure S2**. In both figures, panel A is the double-negative control: in the absence of either TRPM5 or  $\text{TI}^+$ , there is no increase in the fluorescence in Thallos-loaded HEK cells (**Fig. 2A** and **Suppl. Fig. S2A**).

In control HEK cells, the Thallos-dependent fluorescence signal is strongly reduced in  $\text{K}^+$ -based buffers, compared with  $\text{Na}^+$ -based buffers, in both the absence and presence of ionomycin (**Fig. 2B–D** and **Suppl. Fig. S2B–D**). The signal is clearly dependent on the extracellular  $\text{TI}^+$  concentration and is smallest in the presence of 0.2 mM  $\text{TI}^+$ . Furthermore, in  $\text{K}^+$ -based buffers, using aspartate or  $\text{NO}_3^-$  obviously reduces the signal compared with a gluconate-containing buffer (**Fig. 2C,D**). These experiments define what can be considered the “background level” of  $\text{Ca}^{2+}$ -dependent and  $\text{Ca}^{2+}$ -independent  $\text{TI}^+$  influx in HEK cells.

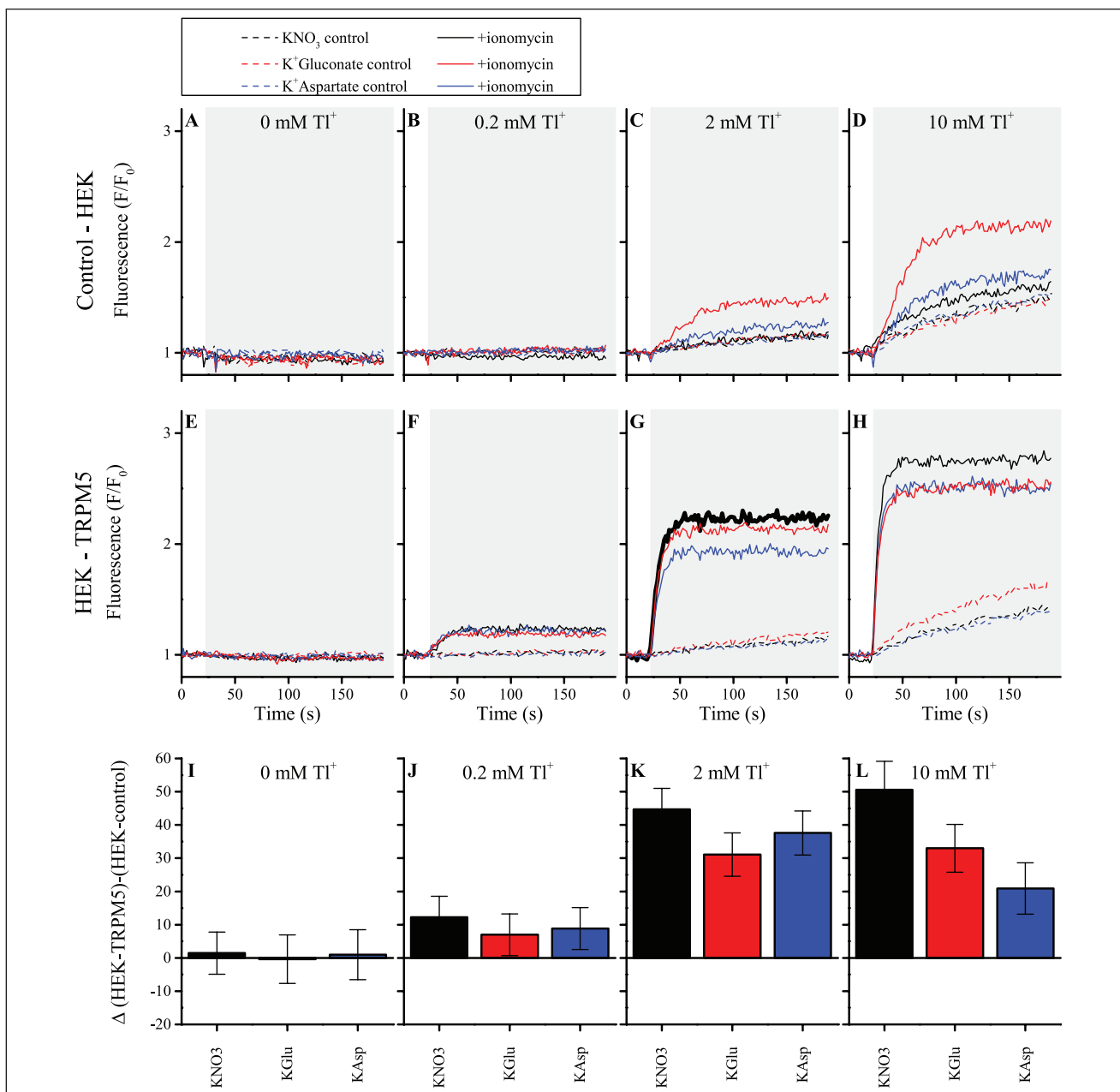


**Figure 2.** Thallium fluorescence increase in K<sup>+</sup> buffers with different anions. The thallium fluorescence measured in the FlexStation3, in each panel, after a 25 s baseline measurement; the appropriate amount of thallium sulfate (0, 0.1, 1, or 5 mM) and ionomycin (0 or 2 μM) is added to the well (gray background), and fluorescence responses were measured for 170 s. (A–D) Traces from wells containing control HEK cells, showing the TRPM5-independent fluorescence increase. (E–H) Traces in the same conditions in HEK cells overexpressing TRPM5. The dashed lines represent control conditions, in the absence of ionomycin, where the solid lines represent the conditions with ionomycin, where TRPM5 is activated. (I–L) The differences in fluorescence amplitude of the ionomycin-induced effect between control HEK cells and HEK TRPM5 cells. A positive value indicates a larger effect of ionomycin in HEK TRPM5 cells.

In HEK TRPM5 cells, the same set of conditions was tested (Fig. 2E–H and Suppl. Fig. 2 SE–H). Application of ionomycin resulted in a sharp increase of fluorescence in all conditions, of which the rate and maximal amplitude were dependent on the Tl<sup>+</sup> concentration and the ions in the buffer. When

comparing K<sup>+</sup>- and Na<sup>+</sup>-based buffers, it is obvious that the reduced background signal in K<sup>+</sup>-based buffers is preferable. Considering the concentration of Tl<sup>+</sup>, the intermediate concentration of 2 mM seems optimal, due to the strong background signal that arises in 10 mM Tl<sup>+</sup> and the fairly limited signal in

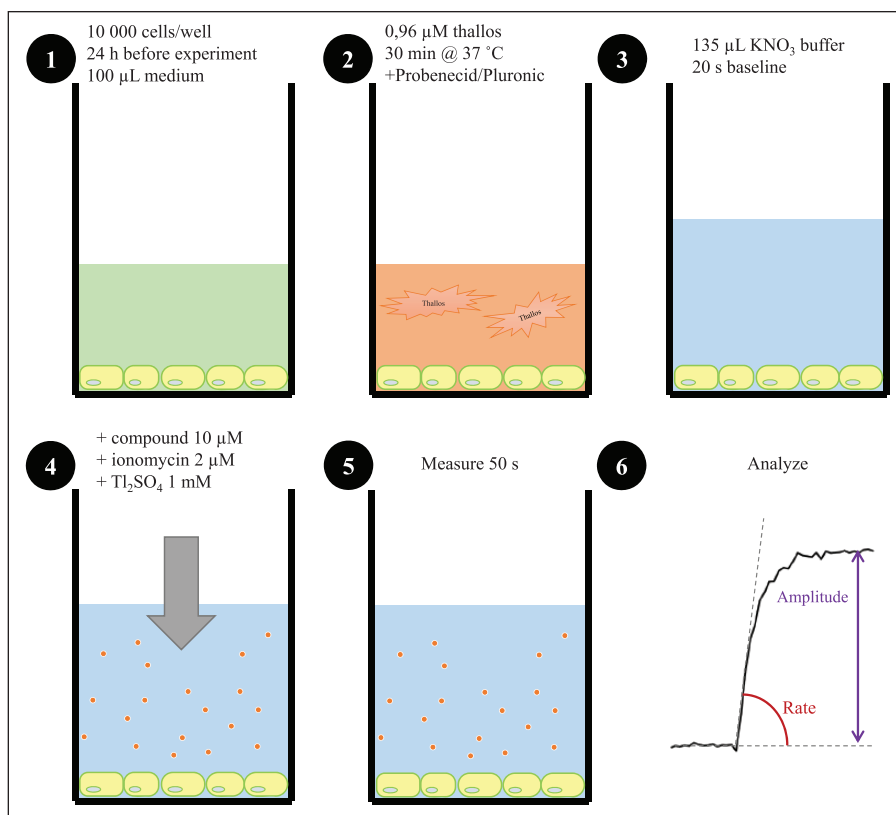


**Figure 3.** Protocol for the compound screening. (1) We seeded 10,000 cells/well in 100  $\mu$ L of medium 24 h before the assay and (2) incubated them for 30 min with 0.96  $\mu$ M Thallos dye with Pluronic F-127 for facilitated uptake and 2.5 mM probenecid. (3) The loading medium was discarded and replaced with 135  $\mu$ L of the  $\text{KNO}_3$ -based assay buffer. After measuring 20 s for baseline, (4) we add 2  $\mu$ M ionomycin, 2 mM thallium, and the compound of interest and (5) follow the fluorescence for 50 s. Compounds were pre-distributed in a 10 $\times$  concentration on 96-well plates, and we transferred 15  $\mu$ L from the compound plate to the 135  $\mu$ L assay buffer in the cell chamber to obtain a 10 $\times$  dilution. (6) Analysis of the fluorescent traces occurs by calculating the amplitude of the fluorescence change and the rate of the fluorescence change, which are normalized to control conditions.

0.2 mM  $\text{TI}^+$  (Fig. 2F–H). Finally, the TRPM5-dependent signal is maximal when  $\text{NO}_3^-$  is used as anion, compared with gluconate or aspartate (Fig. 2G).

In Figure 2I–L and Supplemental Figure S2I–L, the difference in the ionomycin-dependent part of the signal between control HEK cells and HEK TRPM5 cells is shown. Figure 2K shows that the highest TRPM5-dependent signal is observed in a  $\text{KNO}_3$  buffer (black bar). For this reason, this condition was chosen for further screening. Although the signal is slightly higher in the condition with 10 mM  $\text{TI}^+$ , this condition was excluded because of the relatively high aspecific  $\text{TI}^+$  influx. In Supplemental Figure S3, the difference of the signal in  $\text{KNO}_3$  buffer (panel A) compared with that in the  $\text{NaNO}_3$  buffer (panel B) is further highlighted. The figure shows the absolute amplitude, extracted from experiments similar to those shown in Figure 2 and Supplemental Figure S2. In the absence of ionomycin (left), we observed an increase in the (TRPM5-independent) thallium flux with increasing concentrations of  $\text{TI}^+$ . This background signal has a larger amplitude in panel B ( $\text{NaNO}_3$ ) than in panel A ( $\text{KNO}_3$ ). The thallium flux evoked with ionomycin and 1 mM  $\text{Tl}_2\text{SO}_4$  is slightly higher with the  $\text{NaNO}_3$  buffer than the  $\text{KNO}_3$  buffer. However, due to the substantially higher background increase in the  $\text{Na}^+$  condition, the combination of a  $\text{KNO}_3$  buffer and 1 mM  $\text{Tl}_2\text{SO}_4$  (2 mM  $\text{TI}^+$ ) was chosen for further experiments.

Of note, the use of Thallos in these experiments provided a better data separation than a  $\text{Na}^+$ -sensitive dye, such as SBFI, with a signal-to-noise ratio of 37.5 for Thallos compared with 2.9 for SBFI (Suppl. Fig. S4).

### Thallium Influx Is Influenced by Modulating TRPM5

To test whether potentiation or inhibition of TRPM5 activity is detectable with a Thallos-based assay, we made use of the limited amount of known TRPM5 modulators. The assay procedure is illustrated in Figure 3. We used a one-step assay, where the test compound, ionomycin, and  $\text{TI}^+$  were added together to Thallos-loaded cells, and fluorescence was measured for 50 s after application. Immediately upon the addition of ionomycin, the fluorescence increased steeply and a plateau value was reached approximately 20 s later. Both the rate of the fluorescence increase and the maximum amplitude of fluorescence increase were analyzed for each compound (Fig. 3, step 6). In each column of the 96-well plate, a positive control was present: in this condition, only ionomycin and  $\text{TI}^+$  were added. This control was used as the 100% signal in the analysis, and the activity of the compounds was calculated relative to this value.

At a concentration of 10  $\mu$ M, we could confirm the previously reported effect of flufenamic acid (FA), clotrimazole,

and triphenylphosphine oxide (TPPO) on TRPM5 activity (**Suppl. Fig. S5A,B,D,G,H**).<sup>17,34</sup> The inhibitory effect from quinine was not significant at 10  $\mu\text{M}$ , most likely due to the low affinity of quinine (**Suppl. Fig. S5C**).<sup>19</sup> We also confirmed the TRPM5 inhibitory activity of (E)-*N*-(3,4-dimethoxybenzylidene)-2-naphthalene-1-yl)acetohydrazide (ENDNA)<sup>35</sup> and the potentiating effect of SID 2848719 (**Suppl. Fig. S5E–H**).<sup>36</sup> These compounds were described in recent patent applications.<sup>35,36</sup>

The  $Z'$  factor is a window coefficient that provides information about the quality of the assay. It combines the variability and the spread of positive and negative controls to determine the quality of the data for compounds that yield a signal between these control values.<sup>33</sup> We obtained a  $Z'$  factor of 0.89 based on amplitude and 0.71 based on rate of fluorescence change for the assay described in **Supplemental Figure S5**, indicating that the variability within the assay was limited.

Taken together, these results indicate that the Thallo-based assay is capable of reliably identifying compounds modulating TRPM5 activity.

### Thallos-Based Measurement of TRPM4 Activity

Because of the functional similarity between TRPM4 and TRPM5, we also tested the protocol on TRPM4-expressing HEK cells. We optimized the thallium concentrations and ionomycin concentration, similar as above. In **Supplemental Figure S6A,B**, it is shown that the fluorescence increase in TRPM4-expressing cells is dependent on the thallium concentration and on the ionomycin concentration. The highest dynamic range is obtained with 2 mM extracellular thallium and 2  $\mu\text{M}$  ionomycin, and TRPM4-dependent thallium flux into the cell is inhibited by 10  $\mu\text{M}$  clotrimazole (**Suppl. Fig. S6C,D**). These conditions are similar to those for TRPM5, indicating that the protocol optimized for TRPM5 can be applied to screen both channels.

### Limitations of Known TRPM5 Modulators

TRPM5-modulating molecules have been used in several *in vitro* and *ex vivo* studies. Due to the need for high concentrations, the poor solubility of the compounds, and poor selectivity, interpretation of data is often complicated. For instance, FA is described to reduce TRPM5 currents in membrane-delimited inside-out patches.<sup>34</sup> As can be observed in **Figure 4A** at concentrations under 25  $\mu\text{M}$ , FA reduces both the amplitude and rate of fluorescence increase (**Fig. 4A,B**). However, at 50 and 100  $\mu\text{M}$  FA, we observe a slow activating component in the fluorescence trace. Apparently, at these concentrations, a TRPM5-independent influx pathway is activated by FA. Indeed, the maximal fluorescence level at 100  $\mu\text{M}$  FA exceeds the 100% control level (black trace), albeit at a much later time point. The rate of fluorescence

increase is more than 50% reduced, which indicates different kinetics and further supports that TRPM5 is likely not involved in this process. This was confirmed in TRPM5-negative HEK cells, where low concentrations (10  $\mu\text{M}$ ) of FA have no effect (**Suppl. Table S2**) but 100  $\mu\text{M}$  FA clearly activated a thallium influx pathway. Of note, two-pore potassium channels have been reported to be activated by FA and are expressed in HEK cells.<sup>37</sup> In **Figure 4C**, the effect of 10 and 100  $\mu\text{M}$  FA on TRPM4-expressing HEK cells is shown. Again, the inhibiting effect observed at low concentrations, as with TRPM5, was counteracted by increased thallium influx at higher concentrations of FA. 9-Phenanthrol (9-Ph), on the other hand, is widely used as a TRPM4 inhibitor.<sup>38</sup> Application of 9-Ph at a concentration of 10 or 100  $\mu\text{M}$  to the HEK TRPM4 cells in our compound screening revealed a dose-dependent potentiation of the fluorescence signal compared with the control (**Fig. 4D,E**). The lack of apparent inhibitory effect of 9-Ph in the screen may be due to the slow mode of action of 9-Ph and the absence of a washout step in the assay. In this way, delayed inhibition of TRPM4/M5 will not lead to a decrease of the fluorescence signal. It has been reported that 9-Ph could activate  $\text{Ca}^{2+}$ -activated  $\text{K}^+$  channels, but there is no effect of 9-Ph in HEK TRPM5 cells (**Suppl. Table S1**). Taken together, these observations illustrate some caveats of the screening assay that should be considered when searching for new potent and selective TRPM4/5-modulating compounds.

### Screening for TRPM5 Modulators

**Figure 5** illustrates a typical setup of a screening protocol to detect molecules modulating TRPM5 with a high affinity, in a 96-well format. We included a duplicate sample, together with positive and negative controls, allowing 36 unique compounds to be screened per 96-well plate. The concentration of compound used was 10  $\mu\text{M}$ . We randomly added the TRPM5 inhibitor TPPO and potentiator SID 2848719 on a compound plate (**Fig. 5A**) to test whether they can be readily identified (**Fig. 5C,D**). These experiments show that the assay is capable of efficiently identifying TRPM5 modulators among a large number of nonactive compounds. We also analyzed the variability of the positive and negative controls, represented in **Figure 5B**. We observed consistent values for the fluorescence in control conditions over the whole plate, which is reflected in  $Z' = 0.83$ . When analyzing the reproducibility and consistency of the results, we found for SID 2848719,  $Z = 0.79$ , and for TPPO,  $Z = 0.93$ . These values indicate a good dynamic range of the assay and a high signal-to-noise ratio between sample and control conditions.

### Screening of a Library

We assembled a library of 75 compounds with known activity on TRPM5 or other TRP channels, and structurally

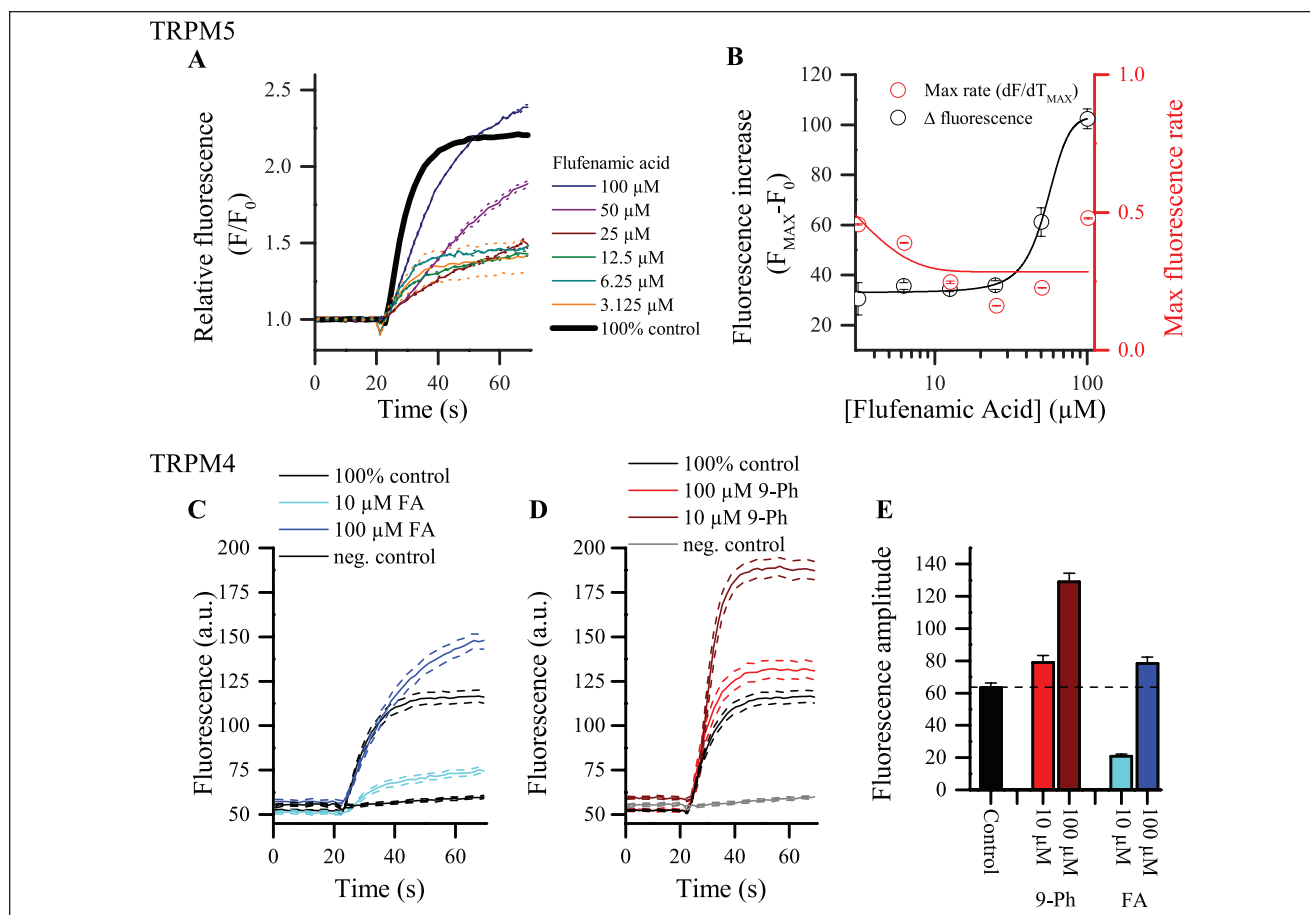


**Figure 4.** Poor selectivity of reported antagonists. **(A)** FA blocks the fluorescence signal in HEK TRPM5 cells (average  $\pm$  SEM of two wells/concentration, 100% control is the average of four wells). The blocking effect of FA is less at higher concentrations. **(B)** We see a dose-dependent increase of the average  $\pm$  SEM maximal amplitude but a decrease of the average  $\pm$  SEM maximal rate of fluorescence increase, indicating a substantial but slow  $\text{Ti}^+$  influx with higher doses of FA. **(C)** In HEK TRPM4 cells, we see similar results as in HEK TRPM5 cells. FA inhibits the TRPM4 activity at lower concentrations, but there is a potentiation of the amplitude of thallium fluorescence at high (100  $\mu\text{M}$ ) concentrations. **(D)** 9-Ph does not inhibit the fluorescence increase in HEK TRPM4 cells; on the contrary, a dose-dependent increase in fluorescence can be observed. **(E)** Average fluorescence increase in HEK TRPM4 cells in control conditions and with 9-Ph or FA at 10 and 100  $\mu\text{M}$ .

related chemicals or other bioactive molecules. The compounds and results are shown in **Supplemental Table S1**. We found TPPO to be the most potent TRPM5 inhibitor in this library. The top six inhibitors based on the rate of fluorescence increase included all known TRPM5 inhibitors and compounds with similar chemical properties. Several azole-based antifungal compounds (clotrimazole, ketoconazole, econazole, and miconazole) inhibit TRPM5 activity. We also detected potentiators of TRPM5 function. Compound SID 2848719 was the top potentiator. If we consider compounds that change both rate and maximum amplitude, the top six potentiators include two steviol glycosides (stevioside and rebaudioside A), together with eugenol, and urea. Quinacrine is a false positive due to its inherent fluorescent properties (**Suppl. Fig. S7C** and **Suppl. Table S1**). The results of this screening confirm the validity

of the assay to pick up TRPM5 modulators among a number of inactive compounds. We obtained an average  $Z'$  factor of  $0.75 \pm 0.01$  based on amplitude changes and  $0.57 \pm 0.03$  based on rate of fluorescence changes. There was good reproducibility of the data, which is reflected in a Pearson's correlation coefficient between replicate measurements of 0.97 based on amplitude and 0.94 based on the rate of fluorescent change.

Both the effect of a compound on rate and the maximal amplitude of the Thallo signal are considered in our analysis.<sup>30</sup> The rate of fluorescence change is directly proportional to the speed of  $\text{Ti}^+$  entering the cell per unit of time, and thus to ion channel conductance. As there is no wash step in the assay,  $\text{Ti}^+$  is not removed from the cell and the amplitude is a measure of cumulative activity and is strongly dependent on the acquisition time, but also the amount of



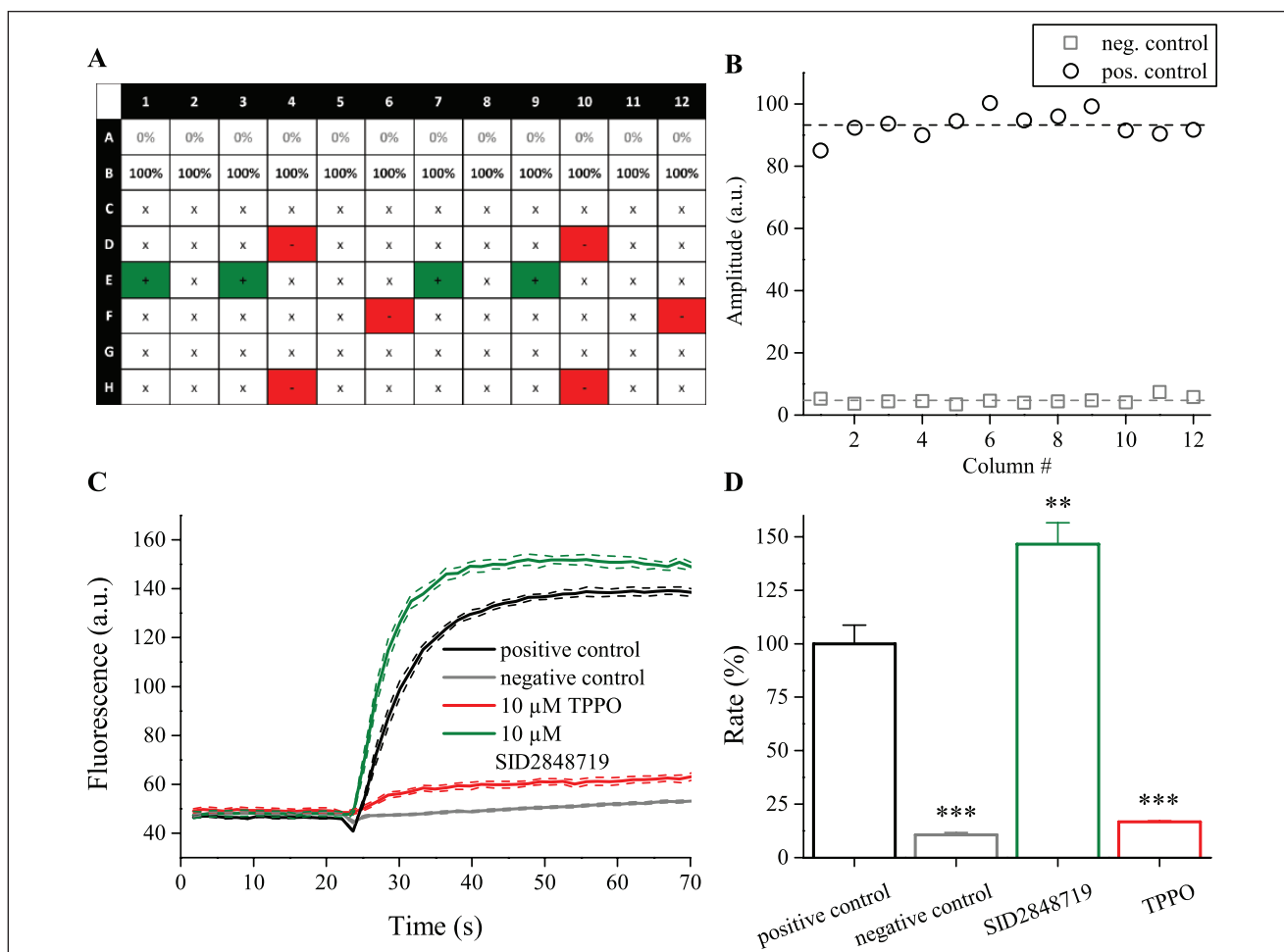


**Figure 5.** Identifying random modulators. **(A)** Layout of a plate that was screened; the positive and negative controls are indicated, as well as the positions of TPPO and SID 2848719. **(B)** Values of the amplitude changes of individual positive and negative controls. **(C)** Average traces of positive control ( $n = 12$ ), negative control ( $n = 12$ ), inhibitor ( $n = 6$ ), and potentiator ( $n = 4$ ). **(D)** Rate of the traces in B.

Thallos in the cell. As seen in **Supplementary Table S1**, in the case of inhibitors there is a good correlation between the effect on rate and amplitude. This is less the case with potentiating compounds. For some compounds, these parameters are qualitatively uncorrelated. For instance, deoxycholic acid increases rate but has no effect on amplitude. FA, on the other hand, strongly inhibits rate but has a more limited effect on amplitude. When these parameters are divergent, the compound likely does not act on TRPM5 but interferes with another step in the assay or another channel. Above, we already illustrated such TRPM5-independent effects for FA. As a rule of thumb, for selection of compounds for further experiments, we thus argue that both rate and amplitude should change to the same extent.

The screening method uses a fluorescence-based readout, which provides that tested compounds do not interfere with fluorescence emission. Possible interference could be either quenching the emitted fluorescence of the dye,

absorbing excitation light, or autofluorescence of the test compound at the examined wavelength. We examined the autofluorescence of all our tested compounds (**Suppl. Table S1** and **Suppl. Fig. S7C**) and identified quinacrine as a false positive.

Simultaneous addition of  $Tl_2SO_4$ , the compound of interest, and ionomycin introduces a bias in the assay. Blockers or potentiators that have a relatively slow onset of action will remain undetected. Also, direct ligands of the channel of interest (i.e., that activate the channel independent of ionomycin) can remain undetected as such. A slower assay (i.e., increased acquisition time after addition of the compound) or a two-step addition protocol (i.e., the compound of interest is added first, and ionomycin and  $Tl_2SO_4$  later) could address this.

Another source of variability in this assay is the possibility that bioactive molecules interfere with ionomycin-induced intracellular calcium increase. Such compounds

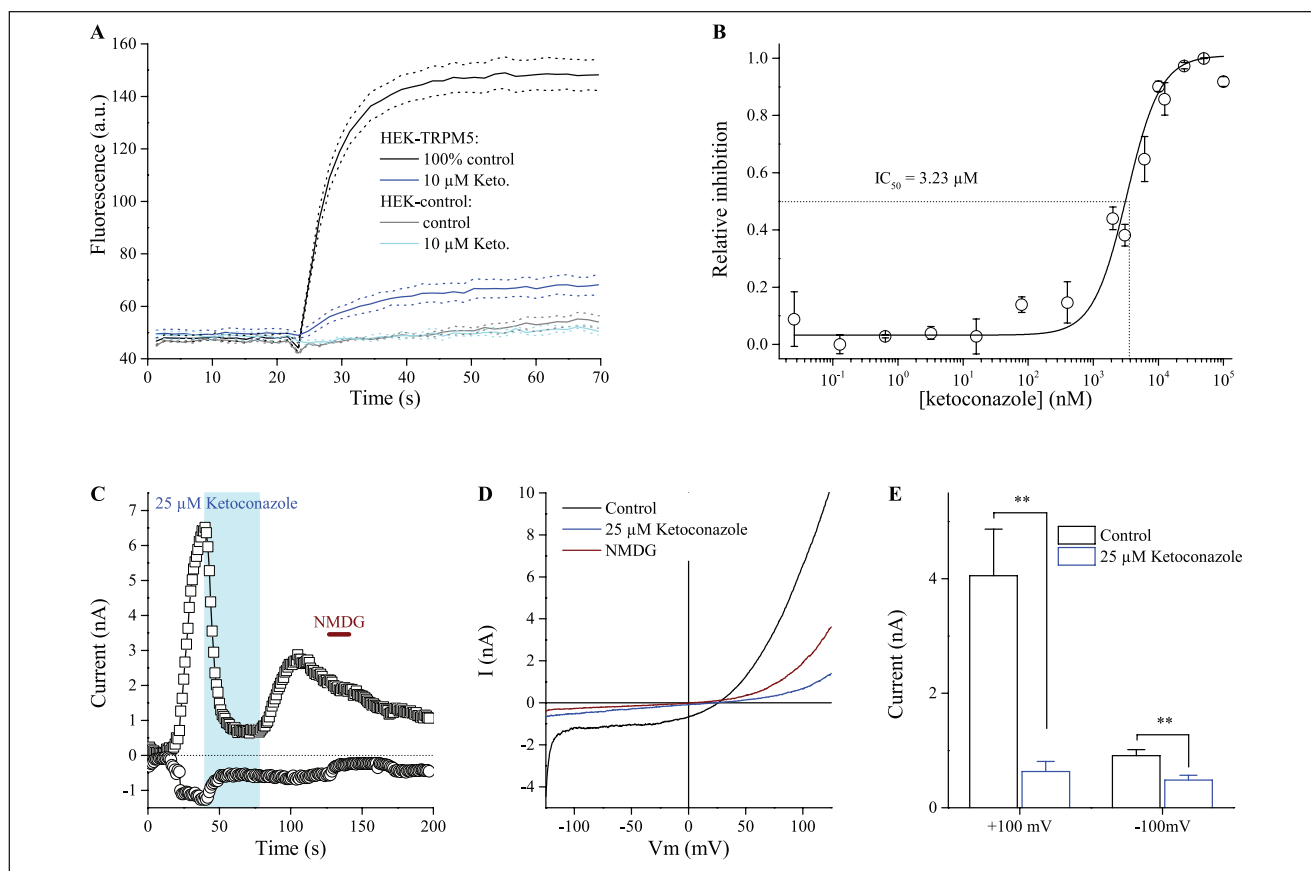


**Figure 6.** Ketoconazole inhibits TRPM5 activity. **(A)** Thallos fluorescence traces of HEK TRPM5 cells (average  $\pm$  SEM of four wells from two independent experiments) and control HEK cells ( $n = 2$  wells) in the presence or absence of 10  $\mu\text{M}$  ketoconazole (added at 20 s). Keto. = ketoconazole. **(B)** Dose–response of the inhibitory effect of ketoconazole on TRPM5 ( $n = 4$  wells/concentration, two individual experiments with a subset of the concentrations). **(C)** Whole-cell patch clamp experiment with 1  $\mu\text{M}$   $[\text{Ca}^{2+}]_i$  and perfusion with 25  $\mu\text{M}$  ketoconazole. The currents are extracted at  $-100$  and  $+100$  mV. **(D)** IV relationship from the time course in C. **(E)** Reduction of the out- and inward currents during patch experiments ( $n = 7$  cells).

are identified by a follow-up screen of initial hit compounds in a FURA2-AM-based assay. In this assay, the intracellular  $\text{Ca}^{2+}$  change is compared between compound and control conditions. The results of this follow-up screening are presented in **Supplemental Figure S7B** and **Supplemental Table S2**. We identify several compounds with autofluorescence at the wavelengths used for excitation of FURA-2. Interference of these compounds (solid circles, **Suppl. Fig. S7B,D**) with  $\text{Ca}^{2+}$  flux cannot be accurately determined. We did, however, observe two compounds (atropine and oxalic acid) that had a significantly lower  $\text{Ca}^{2+}$  increase than the control. These compounds did not change thallium influx in HEK TRPM5 cells.

Screening of the library on both TRPM4 and TRPM5, and on untransfected HEK cells, gives an idea of the specificity of compounds. The Thallos assay on untransfected cells showed increased Thallos fluorescence upon addition of quinacrine (no. 72) and econazole (no. 5) relative to control conditions without compound (**Suppl. Fig. S7A**). As

mentioned above, quinacrine is autofluorescent in this assay. Econazole inhibits TRPM5-dependent thallium flux but increases thallium influx in untransfected HEK cells, which indicates that the inhibitory effect on TRPM5 is likely an underestimation.

### Confirmation Experiments

Despite a range of control experiments, positive hits should be confirmed in an independent assay, preferably via the patch clamp technique. In this study, we further characterized ketoconazole as a TRPM5 inhibitor. Ketoconazole is a synthetic imidazole antifungal agent.<sup>39</sup> It has been used as a systemic fungicide, but its oral use is in decline due to its hepatotoxicity and the availability of less toxic and more effective imidazole compounds. Ketoconazole is still used as the active ingredient for topical administration in the form of a cream or shampoo for the treatment of athlete's foot, seborrheic dermatitis, and androgenic alopecia.<sup>40</sup> In

our screening, 10  $\mu\text{M}$  ketoconazole was shown to inhibit the rate of thallium influx by  $89.7 \pm 2.3\%$  and the maximum amplitude by  $82.9 \pm 4.4\%$  of the positive control. In **Figure 6A**, the average  $\pm$  SEM of four measurements in two independent experiments is shown. We addressed the inhibiting effect at a range of concentrations from 25 pM to 100  $\mu\text{M}$  and observed a dose-dependent block of the TRPM5-mediated thallium influx with an  $\text{IC}_{50}$  of  $3.23 \pm 0.48 \mu\text{M}$  (**Fig. 6B**).

Whole-cell patch clamp studies confirmed the inhibitory effects of ketoconazole on TRPM5-mediated currents. After establishing the whole-cell configuration ( $t = 0$  s), the cell was loaded with 1  $\mu\text{M}$   $\text{Ca}^{2+}$  through the pipette, which activates TRPM5 (**Fig. 6C**). Application of 25  $\mu\text{M}$  ketoconazole significantly reduced in- and outward currents (**Fig. 6C–E**). Recovery upon washout is only partial. When perfusing ketoconazole in the cell-attached phase before establishing the whole-cell configuration, there is an attenuation of the  $\text{Ca}^{2+}$ -induced current until ketoconazole is removed from the bath (**Suppl. Fig. S8**). These experiments confirm that ketoconazole is a TRPM5 inhibitor.

In summary, we developed and optimized an assay for the detection of compounds modulating the activity of the nonselective monovalent cation channels TRPM5 and TRPM4. We used a thallium-sensitive dye and confirmed that  $\text{Tl}^+$  permeates TRPM5 in patch clamp experiments. We show that the screening assay is capable of identifying new compounds that inhibit or activate/potentiate TRPM5 or TRPM4 channel activity. To our knowledge, this is the first assay using a thallium dye to assess the activity of CAN or TRP channels.

### Declaration of Conflicting Interests

The authors declared no potential conflicts of interest with respect to the research, authorship, and/or publication of this article.

### Funding

The authors disclosed receipt of the following financial support for the research, authorship, and/or publication of this article: This work was supported by FWO Vlaanderen (G.0761.10N, G.0596.12, G.0565.07, and G0E0217N), the IUAP program from the Belgian federal government (IcePath, P7/13), and KULeuven “Bijzonder Onderzoeksfonds” (STR1/09/046, GOA 2009/07, EF/95/010, and TRPLe). K.P. received funding from the European Union’s Horizon 2020 research and innovation program under Marie Skłodowska-Curie grant agreement no. 665501 with the research Foundation Flanders (FWO) as an FWO [PEGASUS]<sup>2</sup> Marie Skłodowska-Curie Fellow. This article was published with the support of the University Foundation Belgium.

### ORCID iD

Koenraad Philippaert  <https://orcid.org/0000-0002-5861-2275>

### References

1. Prawitt, D.; Monteilh-Zoller, M. K.; Brixel, L.; et al. TRPM5 Is a Transient  $\text{Ca}^{2+}$ -Activated Cation Channel Responding to Rapid Changes in  $[\text{Ca}^{2+}]_i$ . *Proc. Natl. Acad. Sci. U.S.A.* **2003**, *100*, 15166–15171.
2. Colsoul, B.; Kecskes, M.; Philippaert, K.; et al. The  $\text{Ca}^{2+}$ -Activated Monovalent Cation-Selective Channels TRPM4 and TRPM5. In *TRP Channels in Drug Discovery: Methods in Pharmacology and Toxicology*; Szallasi, A., Biró, T., Eds.; Humana Press: Totowa, NJ, **2012**; Vol. 1, pp 103–125.
3. Colquhoun, D.; Neher, E.; Reuter, H.; et al. Inward Current Channels Activated by Intracellular Ca in Cultured Cardiac Cells. *Nature* **1981**, *294*, 752–754.
4. Launay, P.; Fleig, A.; Perraud, A. L.; et al. TRPM4 Is a  $\text{Ca}^{2+}$ -Activated Nonselective Cation Channel Mediating Cell Membrane Depolarization. *Cell* **2002**, *109*, 397–407.
5. Mathar I.; Jacobs G.; Kecskes M.; et al. TRPM4. In *Mammalian Transient Receptor Potential (TRP) Cation Channels*; Nilius, B., Flockerzi, V., Eds.; Handbook of Experimental Pharmacology; Springer: Berlin, Germany, **2014**, pp. 461–487.
6. Vennekens, R.; Olausson, J.; Meissner, M.; et al. Increased IgE-Dependent Mast Cell Activation and Anaphylactic Responses in Mice Lacking the Calcium-Activated Nonselective Cation Channel TRPM4. *Nat. Immunol.* **2007**, *8*, 312–320.
7. Kruse, M.; Schulze-Bahr, E.; Corfield, V.; et al. Impaired Endocytosis of the Ion Channel TRPM4 Is Associated with Human Progressive Familial Heart Block Type I. *J. Clin. Invest.* **2009**, *119*, 2737–2744.
8. Zhang, F.; Klebansky, B.; Fine, R. M.; et al. Molecular Mechanism of the Sweet Taste Enhancers. *Proc. Natl. Acad. Sci. U.S.A.* **2010**, *107*, 4752–4757.
9. Stallmeyer, B.; Zumhagen, S.; Denjoy, I.; et al. Mutational Spectrum in the  $\text{Ca}^{2+}$ -Activated Cation Channel Gene TRPM4 in Patients with Cardiac Conductance Disturbances. *Hum. Mutat.* **2012**, *33*, 109–117.
10. Colsoul, B.; Schraenen, A.; Lemaire, K.; et al. Loss of High-Frequency Glucose-Induced  $\text{Ca}^{2+}$  Oscillations in Pancreatic Islets Correlates with Impaired Glucose Tolerance in *Trpm5*<sup>−/−</sup> Mice. *Proc. Natl. Acad. Sci. U.S.A.* **2010**, *107*, 5208–5213.
11. Philippaert, K.; Pironet, A.; Mesuere, M.; et al. Steviol Glycosides Enhance Pancreatic Beta-Cell Function and Taste Sensation by Potentiation of TRPM5 Channel Activity. *Nat. Commun.* **2017**, *8*, 14733.
12. Wilmot, E.; Idris, I. Early Onset Type 2 Diabetes: Risk Factors, Clinical Impact and Management *Ther. Adv. Chronic Dis.* **2014**, *5*, 234–244.
13. Kaske, S.; Krasteva, G.; König, P.; et al. TRPM5, a Taste-Signaling Transient Receptor Potential Ion-Channel, Is a Ubiquitous Signaling Component in Chemosensory Cells. *BMC Neurosci.* **2007**, *8*, 49.
14. Liu, D.; Liman, E. R. Intracellular  $\text{Ca}^{2+}$  and the Phospholipid PIP2 Regulate the Taste Transduction Ion Channel TRPM5. *Proc. Natl. Acad. Sci. U.S.A.* **2003**, *100*, 15160–15165.
15. Pérez, C. A.; Huang, L.; Rong, M.; et al. A Transient Receptor Potential Channel Expressed in Taste Receptor Cells. *Nat. Neurosci.* **2002**, *5*, 1169–1176.

16. Chandrashekar, J.; Hoon, M. A.; Ryba, N. J. P.; et al. The Receptors and Cells for Mammalian Taste. *Nature* **2006**, *444*, 288–294.
17. Palmer, R. K.; Atwal, K.; Bakaj, I.; et al. Triphenylphosphine Oxide Is a Potent and Selective Inhibitor of the Transient Receptor Potential Melastatin-5 Ion Channel. *Assay Drug Dev. Technol.* **2010**, *8*, 703–713.
18. Ullrich, N. D. TRPM4 and TRPM5: Functional Characterization and Comparison of Two Novel Ca<sup>2+</sup>-Activated Cation Channels of the TRPM Subfamily TRPM4 and TRPM5; KULeuven: Leuven, Belgium, **2005**.
19. Talavera, K.; Yasumatsu, K.; Yoshida, R.; et al. The Taste Transduction Channel TRPM5 Is a Locus for Bitter-Sweet Taste Interactions. *FASEB J.* **2008**, *22*, 1343–1355.
20. Gees, M.; Alpizar, Y. A.; Luyten, T.; et al. Differential Effects of Bitter Compounds on the Taste Transduction Channels TRPM5 and IP3 Receptor Type 3. *Chem. Senses* **2014**, *39*, 295–311.
21. Mancuso, G.; Boronovo, G.; Scaglioni, L.; et al. Phytochemicals from *Ruta graveolens* Activate TAS2R Bitter Taste Receptors and TRP Channels Involved in Gustation and Nociception. *Molecules* **2015**, *20*, 18907–18922.
22. Vennekens, R.; Mesuere, M.; Philippaert, K. TRPM5 in the Battle against Diabetes and Obesity. *Acta Physiol.* **2017**. DOI: 10.1111/apha.12949.
23. Luo, J.; Zhu, Y.; Zhu, M. X.; et al. Cell-Based Calcium Assay for Medium to High Throughput Screening of TRP Channel Functions Using FlexStation 3. *J. Vis. Exp.* **2011**, *e3149*, 1–6.
24. Miller, M.; Wu, M.; Xu, J.; et al. High-Throughput Screening of TRPC Channel Ligands Using Cell-Based Assays. In *TRP Channels*; Zhu, M. X., Ed.; CRC Press: Boca Raton, FL, **2011**; pp 1–14.
25. Zicha, S.; Radresa, O.; Laplante, P.; et al. Novel Methodology to Identify TRPV1 Antagonists Independent of Capsaicin Activation. *J. Biomol. Screen.* **2013**, *18*, 544–555.
26. Reubish, D.; Emerling, D.; Defalco, J.; et al. Functional Assessment of Temperature-Gated Ion-Channel Activity Using a Real-Time PCR Machine. *Biotechniques* **2009**, *47*, iii–ix.
27. Castillo, B.; Pörzgen, P.; Penner, R.; et al. Development and Optimization of a High-Throughput Bioassay for TRPM7 Ion Channel Inhibitors. *J. Biomol. Screen.* **2010**, *15*, 498–507.
28. Bryant, R. W.; Lee, S. P.; Palmer, R. K.; et al. High Throughput Screening Assay for the TRPM5 Ion Channel. CA2626852 A1, **2007**.
29. Jørgensen, S.; Dyhring, T.; Brown, D. T.; et al. A High-Throughput Screening Campaign for Detection of Ca<sup>2+</sup>-Activated k(+) Channel Activators and Inhibitors Using a Fluorometric Imaging Plate Reader-Based Tl(+)-Influx Assay. *Assay Drug Dev. Technol.* **2013**, *11*, 163–172.
30. Raphemot, R.; Weaver, C. D.; Denton, J. S. High-Throughput Screening for Small-Molecule Modulators of Inward Rectifier Potassium Channels. *J. Vis. Exp.* **2013**, 1–8.
31. Du, Y.; Days, E.; Romaine, I.; et al. Development and Validation of a Thallium Flux-Based Functional Assay for the Sodium Channel NaV1.7 and Its Utility for Lead Discovery and Compound Profiling. *ACS Chem. Neurosci.* **2015**, *6*, 871–878.
32. Weaver, C. D.; Harden, D.; Dworetzky, S. I.; et al. A Thallium-Sensitive, Fluorescence-Based Assay for Detecting and Characterizing Potassium Channel Modulators in Mammalian Cells. *J. Biomol. Screen.* **2004**, *9*, 671–677.
33. Zhang, J. H.; Chung, T. D.; Oldenburg, K. R. A Simple Statistical Parameter for Use in Evaluation and Validation of High Throughput Screening Assays. *J. Biomol. Screen.* **1999**, *4*, 67–73.
34. Ullrich, N. D.; Voets, T.; Prenen, J.; et al. Comparison of Functional Properties of the Ca<sup>2+</sup>-Activated Cation Channels TRPM4 and TRPM5 from Mice. *Cell Calcium* **2005**, *37*, 267–278.
35. Lee, S. P.; Zhou, P.; Buber, N. T.; et al. Use of a TRPM5 Inhibitor to Regulate Insulin and GLP-1 Release. Google Patents 2008.
36. Servant, G.; Williams, M.; Patron, A.; et al. TRPM5 Based Assays and the Use Thereof for the Identification of Modulators of Sweet, Bitter or Umami (Savory) Taste. *Google Patents 2007*.
37. Guinamard, R.; Simard, C.; Del Negro, C. Flufenamic Acid as an Ion Channel Modulator. *Pharmacol. Ther.* **2013**, *138*, 272–284.
38. Guinamard, R.; Hof, T.; Del Negro, C. A. The TRPM4 Channel Inhibitor 9-Phenanthrol. *Br. J. Pharmacol.* **2014**, *171*, 1600–1613.
39. Fromtling, R. A. Overview of Medically Important Antifungal Azole Derivatives. *Clin. Microbiol. Rev.* **1988**, *1*, 187–217.
40. McElwee, K. J.; Shapiro, J. S. Promising Therapies for Treating and/or Preventing Androgenic Alopecia. *Skin Therapy Lett.* **2012**, *17*, 1–4.